Surface & Coatings Technology 209 (2012) 203–207

Contents lists available at SciVerse ScienceDirect

Surface & Coatings Technology

journal homepage: www.elsevier.com/locate/surfcoat

Pressure and temperature effects on the decomposition of arc evaporated $Ti_{0.6}Al_{0.4}N$ coatings in continuous turning

N. Norrby [a,*], M.P. Johansson [a,b], R. M'Saoubi [b], M. Odén [a]

[a] Nanostructured Materials, Department of Physics, Chemistry and Biology (IFM), Linköping University, SE-58183 Linköping, Sweden
[b] R&D Material and Technology Development, Seco Tools AB, SE-73782 Fagersta, Sweden

ARTICLE INFO

Article history:
Received 19 March 2012
Accepted in revised form 28 August 2012
Available online 4 September 2012

Keywords:
Spinodal decomposition
Metal cutting
High stresses

ABSTRACT

The isostructural decomposition of arc evaporated $Ti_{0.6}Al_{0.4}N$ coatings at elevated temperatures and high stresses occurring during metal cutting has been studied. Comparisons are made with short time (t = 10 min) anneals at temperatures typical for steel turning operations. The evolution of the spinodal wavelengths is studied by analytical transmission electron microscopy from samples originating from the rake face. Temperature and force measurements during turning allowed for separation of the effects of the temperature and stresses on wavelength evolution. The results show a peak temperature of around 900 °C and a peak normal stress of around 2 GPa during cutting. The overall wavelength is longer after cutting compared to the annealed sample at the same temperature. The results suggest that pressures generated during cutting promote coherent isostructural decomposition which is in line with theoretical studies but for considerably higher pressures.

1. Introduction

Industrially important since the 1990s [1,2], $Ti_{1-x}Al_xN$ is a widely used physical vapor deposited hard coating with superior high temperature properties compared to its predecessor TiN. A contributor to this is the observed age hardening during annealing, which is an effect of the decomposition of the as-deposited unstable cubic (*c*)-$Ti_{1-x}Al_xN$ (B1) structure into nanometer sized *c*-TiN rich and *c*-AlN rich coherent domains [3,4]. The lattice mismatch between the coherent domains introduces microstresses at the domain borders which in combination with evolving elastic property differences hinder dislocation motion [5]. As ab initio calculations [6] are showing a miscibility gap with a negative second derivative of the Gibb's free energy for the $Ti_{1-x}Al_xN$ solid solution, this step is considered a spinodal decomposition. Upon further annealing, the TiN domains are enriched while *c*-AlN transforms to its stable wurtzite (*w*) phase (B4, *w*-AlN), which detrimentally reduces the mechanical properties of the coating [7].

Recent theoretical studies show that an external pressure will thermodynamically promote the spinodal decomposition [8] and suppress the *c*-AlN to *w*-AlN transformation [8,9]. Reasons for this include the deviation from Vegard's law and the pressure dependent stability of *c*-AlN. Based on this study [8], the effect of pressure is believed to be more distinct at Al compositions around 0.4 due to a shoulder of the spinodal region in the isostructural phase diagram of $Ti_{1-x}Al_xN$. Since not only high temperatures [10,11] but also high stresses prevail at the rake face [12,13] of an insert during cutting, it is suspected that cutting operations are likely to give an even more pronounced spinodal decomposition compared to isothermal anneals.

Although several studies previously reported on the decomposition of post annealed $Ti_{1-x}Al_xN$ [3,7,14], a detailed study of the $Ti_{1-x}Al_xN$ decomposition at the cutting edge is still lacking. This is the motive of the present study where the microstructure evolution of $Ti_{0.6}Al_{0.4}N$ after cutting was compared to reference heat treatments performed with isothermal steps of 10 min. Microstructure and local chemistry at different positions along the rake face of the cutting insert, i.e., at sample positions exposed to different stresses and temperatures during the cutting process were investigated by analytical transmission electron microscopy (TEM). The evolution of the spinodal decomposition is later discussed in terms of the temperature and stress distributions.

2. Experimental details

A commercial Sulzer Metaplas MZR323 reactive cathodic arc evaporation system was used to deposit the coatings in a 4.5 Pa N_2 atmosphere, substrate temperature ~500 °C with a bias of −40 V. Polished WC–Co cutting inserts (ISO geometry TPUN160308) and blanks (ISO SNUN120408) were used as substrates that were ultrasonically cleaned and Ar-ion etched prior to the coating process. The substrates were mounted on a rotating drum (substrate holder) facing the cathodes placed in line and at different heights on the side wall of the deposition chamber. With this configuration, coatings with different chemical compositions can be deposited by combining different cathodes. In this work, we deposited a $Ti_{0.6}Al_{0.4}N$ composition by using a pure Ti cathode in combination with a compound $Ti_{0.50}Al_{0.50}$ cathode mounted in two positions at different heights in

* Corresponding author. Tel.: +46 13282907; fax: +46 13288918.
E-mail address: nikno@ifm.liu.se (N. Norrby).

0257-8972/$ – see front matter © 2012 Elsevier B.V. All rights reserved.
http://dx.doi.org/10.1016/j.surfcoat.2012.08.068

the chamber. Energy dispersive X-ray spectroscopy (EDS) was employed to verify the coating composition using a Leo 1550 Gemini scanning electron microscope operated at a working distance of 10 mm and using 20 kV.

The machining experiments consisted of dry longitudinal turning in a carbon steel, C45E (yield stress of 280 MPa, rupture stress of 590–740 MPa and hardness of 165–220 HB), with a cutting speed (v_c) of 200 m/min, feed (f) 0.3 mm/rev, depth of cut (a_p) 3 mm and time in cut of 10 min. Additionally, dry orthogonal cutting tests were performed to measure the cutting forces using a standard three-force component dynamometer and the tool temperature distribution was measured using an IR-CCD camera as described by M'Saoubi et al. [15]. The temperature measurements were performed using a cutting time of 10–15 s. The information of the cutting forces together with cutting parameters including chip thickness, work material shear strength and contact length are further introduced in an analytical model [16] for calculation of the normal and tangential stress distribution along the rake face.

For comparison, part of the coatings were annealed in vacuum (base pressure $<3\cdot10^{-5}$ Torr) with a heating rate of 20 °C/min up to T_{max} (900 and 1000 °C) where the coatings were held isothermally for 10 min before a cool down with 50 °C/min. Prior to annealing, samples were cut in small pieces, $1.7\times0.5\times0.5$ mm^3 in order to minimize thermal gradients.

Structural characterizations were performed with a Fei Tecnai G^2 TF 20 UT analytical transmission electron microscope (TEM and STEM) operated at an acceleration voltage of 200 kV and equipped with an energy dispersive X-ray spectrometer (EDS). STEM imaging was performed with a high angle annular detector at a camera length of 170 mm.

TEM sample preparation on the rake face of the coated insert, after machining, was performed using a Carl Zeiss CrossBeam 1540 EsB focused ion beam (FIB) to create cross sectional samples with the lift out technique described in [17]. Cross sectional TEM sample preparation for annealed samples was performed by mechanical grinding and polishing followed by thinning to electron transparency with a Gatan Precision Ion Polishing System.

The spinodal wavelengths have been extracted from STEM micrograph using the line profile tool in the Gatan Digital Micrograph. Several line profiles in the micrographs have been performed from where an average of the sinusoidal gray scale intensity variations has been calculated.

3. Results and discussion

3.1. Temperature and stress distribution

Fig. 1(a) shows the temperature distribution of a cutting tool insert during turning at $v_c=200$ m/min. The insert is viewed from the side with the chip sliding along the rake face on the left side where the tool-chip contact length is marked with an arrow. Fig. 1(b) shows the temperature profile along the contact length, with temperatures between 700 °C and 900 °C. The moderate temperature at the cutting edge increases sharply to a nearly constant value of 850–900 °C across a 0.5 mm wide region. Further away the temperature decreases. The highest temperature is observed at about half the contact length, hereinafter referred to as the hot zone where the maximum temperature, T_{max}, is measured to 890 °C. Both the distribution and the magnitude of the temperature profile are consistent with previous studies [15,18,19].

Fig. 2 shows the normal and tangential stress distributions along the rake face at $v_c=200$ m/min. The normal stress has its maximum of about 2 GPa at the cutting edge and monotonically decreases with increasing distance from the cutting edge. The tangential stress distribution starts with a low value of about 0.4 GPa at the cutting edge and increases up to its maximum value of about 0.8 GPa at half the contact length after which it decreases further away from the cutting edge. Both the magnitude and relative values of the normal and tangential stresses are in reasonable agreement with previous studies which show peak normal stresses of ~2 GPa and peak tangential stresses of ~0.7 GPa [11]. An error margin is estimated to be 15%, taking into account the standard deviation of the cutting forces and measurement errors. In addition, the inset shows the rake face of a worn cutting insert with an arrow indicating the line along which the relative distance from the cutting edge was measured. The letters A–D describe the relative positions along this line from which TEM samples have been obtained.

3.2. Microstructure evolution

Fig. 3(a–c) shows cross sectional overview TEM micrographs of $Ti_{0.6}Al_{0.4}N$ coatings in its as-deposited state, after cutting and after annealing, respectively. For the as-deposited coating, the micrograph reveals a dense columnar structure with a column width around 500 nm and a high defect density typical for arc evaporated $Ti_{0.6}Al_{0.4}N$. The defect density is clearly reduced after cutting and annealing, suggesting that defect annihilation has taken place despite the relatively short exposure time of 10 min during either the annealing or the cutting experiments.

Fig. 4(a–c) shows cross sectional STEM, Z-contrast, micrographs of the $Ti_{0.6}Al_{0.4}N$ layers in its as-deposited state and after annealing to 900 and 1000 °C. The *c*-TiN-rich areas appear with a brighter contrast and *c*-AlN-rich areas with darker contrast (confirmed by EDS mapping but not shown). In its as-deposited state, Fig. 4(a), the Z-contrast image reveals a small layered modulation in composition. This layering effect stems from the rotation of the inserts during the deposition process as described by Eriksson et al. [20]. After annealing, Fig. 4(b and c)

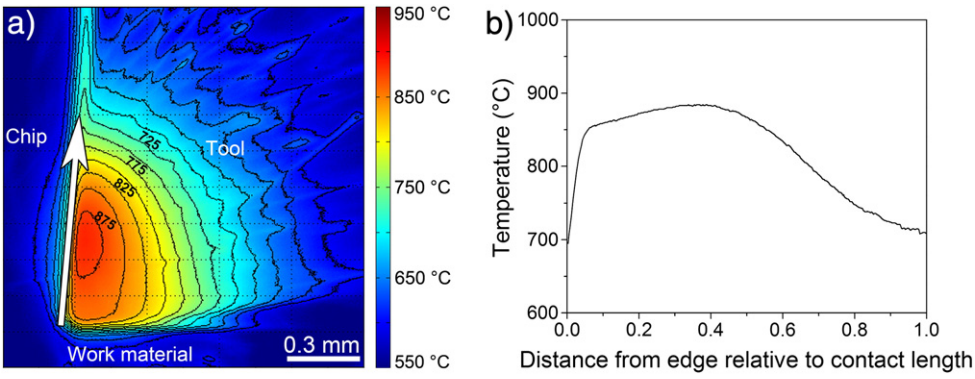

Fig. 1. a) Side view of the temperature distribution as measured by the IR-CCD camera during cutting with cutting speed of 200 m/min. The arrow indicates the distance from the cutting edge and the position of the temperature extraction shown in b).